# Supporting information

# Limits of Activity: Weakly Coordinating Ligands in Arylphosphinesulfonato Palladium(II) Polymerization Catalysts

*Boris Neuwald, Franz Ölscher, Inigo Göttker-Schnetmann and Stefan Mecking**

Chair of Chemical Materials Science, Department of Chemistry, University of Konstanz, 78464 Konstanz, Germany
Fax: +49 7531 88-5152; Tel: +49 7531 88-5151

**Contents:**

## I. Materials and general considerations

Unless noted otherwise, all manipulations of air sensitive compounds were carried out under an inert atmosphere using standard glovebox or Schlenk techniques. THF, Toluene, $CH_2Cl_2$ and MeOH were dried using standard protocols.[1] Pentane and $Et_2O$ were dried by passing through columns equipped with aluminum oxide/molecular sieve 3Å. Ethylene (3.5 grade) supplied by Praxair and methyl acrylate (99%) supplied by Aldrich were used as received. [(tmeda)$PdMe_2$][2], [(cod)PdMeCl][3], 2-[bis(2-methoxyphenyl)phosphino]benzenesulfonic acid[4], **1-dmso**,[5] and [{(**1-Cl**)-μ-Na}$_2$][6] were prepared by known procedures. NMR spectra were recorded on a Varian Unity INOVA 400, a Bruker Avance DRX 600 or a Bruker Avance III 600 spectrometer, equipped with a cryoprobe head. $^1$H and $^{13}$C NMR chemical shifts were referenced to the solvent signal. $^{19}$F and $^{31}$P NMR chemical shifts were referenced to $CFCl_3$ and 85% $H_3PO_4$, respectively. Multiplicities are given as follows (or combinations thereof): s: singlet, d: doublet, t: triplet, vt: virtual triplet, m: multiplet. The identity and purity of metal complexes was established by $^1$H, $^{13}$C and $^{31}$P NMR, and elemental analysis. NMR assignments were confirmed by $^1$H,$^1$H gCOSY, $^1$H,$^{13}$C gHSQC and $^1$H,$^{13}$C gHMBC experiments. For copolymers molecular weights were determined by $^1$H-NMR and the polydispersity index was determined by GPC on a polymer laboratories PL-GPC 50 instrument with two PLgel 5 μm MIXED-C columns and an RI-detector in THF against polystyrene standard. Elemental analysis and FAB mass spectra were obtained by the Analytical Services at the Department of Chemistry, University of Konstanz. Elemental analyses were performed on an Elementar vario MICRO cube instrument. FAB mass spectra were obtained with a double-focusing Finnagan MAT 8200 mass spectrometer equipped with a Ion Tech (Teddington, U.K) FAB Ion Source. ESI mass spectra were recorded on a Bruker Esquire 3000+ instrument.

## II. Synthetic Procedures

### General procedure for the synthesis of phosphine oxides:

To a solution of the corresponding phosphine in THF an excess aqueous $H_2O_2$ (30%) was added. The reaction mixture was stirred for 2 hours at 25 °C. To the solution was added $MnO_2$ and the reaction mixture was heated for 15 min. After cooling to 25 °C the reaction mixture was filtered over Celite® and the filtrate was evaporated under vacuum. The resulting solid was purified as denoted.

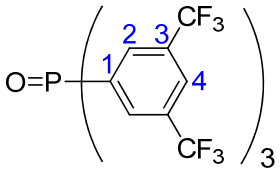


*O=P(C$_7$H$_3$F$_6$)$_3$;* ***OP(3,5-(CF$_3$)$_2$C$_6$H$_3$)$_3$:*** Further purification was not necessary. OP(3,5-$(CF_3)_2C_6H_3)_3$ was obtained as a white solid (306 mg, 0.5 mmol, 66 %)

**$^1$H-NMR** (400 MHz, $CD_2Cl_2$): δ = 8.22 (3H, 4-H), 8.16 (d, $^3J_{PH}$ = 12.1 Hz, 6H, 2-H). **$^{13}$C{$^1$H}-NMR** (101 MHz, $CDCl_3$): δ = 133.8 (d, $^1J_{CP}$ = 105.6 Hz, C1), 133.6 (qd, $^2J_{CF}$ = 34.3 Hz, $^3J_{CP}$ = 12.7 Hz, C3), 132.7-132.4 (m, C2), 128.0 (dq, $^4J_{CP}$ = 7.0 Hz, $^3J_{CF}$ = 3.4 Hz, C4), 123.2 (q, $^1J_{CF}$ = 273.0 Hz, *C*$F_3$). **$^{31}$P{$^1$H}-NMR** (162 MHz, $CDCl_3$): δ = 21.4. **$^{19}$F{$^1$H}-NMR** (377 MHz, $CDCl_3$): δ = -63.5. **Anal. Calcd.** (%) for ($C_{24}H_9F_{18}OP$): C, 42.00; H, 1.32; Found: C, 41.95; H, 1.42. **ATR-IR:** 1/λ [cm$^{-1}$] = 1622 (w), 1607 (w), 1361 (m), 1278(s), 1216 (m, *ν*(P=O)), 1173 (m), 1136 (s), 1121 (ss), 1097 (s), 903 (m), 837 (m), 701 (s), 681 (s). **MS(FAB):** *m/z* = 687 $[M+H]^+$.

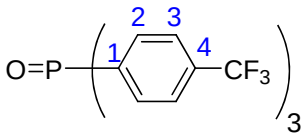


*O=P(C₇H₄F₃)₃;* ***OP(p-CF₃C₆H₄)₃****:* The crude product was washed with pentane and dried under vacuum to yield OP(*p*-$CF_3C_6H_4)_3$ as a white solid (532 mg, 1.1 mmol, 91%).

**$^1$H-NMR** (400 MHz, $CD_2Cl_2$): δ = 7.86-7.77 (m, 12H, 2-H & 3-H). **$^{13}$C{$^1$H}-NMR** (101 MHz, $CD_2Cl_2$): δ = 136.4 (d, $^1J_{CP}$ = 103.3, C1), 134.7 (q, $^2J_{CF}$ = 35.7, C4), 133.1 (d, $^2J_{CP}$ = 10.3, C2), 126.3 (dq, $^3J_{CP}$ = 11.8, $^3J_{CF}$ = 3.7, C3), 124.2 (q, $^1J_{CF}$ = 272.3 Hz, *C*$F_3$). **$^{31}$P{$^1$H}-NMR** (162 MHz, $CDCl_3$): δ = 24.5. **$^{19}$F{$^1$H}-NMR** (377 MHz, $CDCl_3$): δ = -63.7. **Anal. Calcd.** (%) for ($C_{21}H_{12}F_9OP$): C, 52.30; H, 2.51; Found: C, 52.28; H, 2.66. **ATR-IR:** 1/λ [$cm^{-1}$] = 1611(w), 1505 (w), 1402 (m), 1322(ss), 1198 (m, *ν*(P=O)), 1165 (s), 1123(s), 1110(s), 1061 (ss), 1018 (s), 834 (s), 710 (ss). **MS(FAB):** *m/z* = 483 $[M+H]^+$.

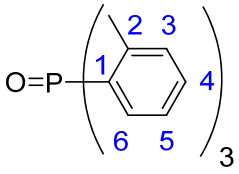


*O=P(C₇H₇)₃;* ***OP(o-Tol)₃****:* The crude product was washed with pentane and dried under vacuum to yield OP(*o*-Tol)$_3$ as a white solid (196 mg, 0.6 mmol, 34%).

**$^1$H-NMR** (400 MHz, $CDCl_3$): δ = 7.43 (vt, *J* = 7.4 Hz, 3H, 4-H), 7.31 (dd, $^3J_{HH}$ = 7.3, $^4J_{PH}$ = 4.0 Hz, 3H, 3-H), 7.17 – 7.06 (m, 6H, 5-H & 6-H), 2.50 (s, 9H, Me). **$^{13}$C{$^1$H}-NMR** (101 MHz, $CDCl_3$): δ = 143.7 (d, $^2J_{CP}$ = 7.7 Hz, C2), 133.0 (d, $^2J_{CP}$ = 12.7 Hz, C6), 132.1 (d, $^3J_{CP}$ = 10.4 Hz, C3), 131.9 (d, $^4J_{CP}$ = 2.6 Hz, C4), 130.9 (d, $^1J_{CP}$ = 101.2 Hz, C1), 125.6 (d, $^3J_{CP}$ = 12.8 Hz, C5), 22.1 (d, $^3J_{CP}$ = 4.0 Hz, Me). **$^{31}$P{$^1$H}-NMR** (162 MHz, $CDCl_3$): δ = 37.0. **Anal. Calcd.** (%) for ($C_{21}H_{21}OP$): C, 78.73; H, 6.61; Found: C, 78.90; H, 6.79. **ATR-IR:** 1/λ [$cm^{-1}$] = 3062 (w), 2958 (w), 2922 (w), 1591(w) 1566 (w), 1450(m), 1279 (m), 1185 (s, *ν*(P=O)), 1162 (m), 1136 (s), 1083 (m), 807 (s), 770 (s), 754 (ss), 719 (ss), 686 (ss). **MS(FAB):** *m/z* = 321 $[M+H]^+$.

## III. Coordination Equilibria

### Equilibrium constants of [(P^O)PdMe(dmso)] + L ⇆ [(P^O)PdMe(L)] + dmso

$^1$H-NMR experiments were performed to study the coordination strength of dmso in comparison to various phosphine oxides.

Standard procedure: 5.2 mg (8.6 µmol) **1-dmso** were weighed in a NMR tube and dissolved in 0.55 mL $CD_2Cl_2$ (c = 1.6 x $10^{-2}$ mol $L^{-1}$). A $^1$H-NMR spectrum was recorded to determine the shift of the O=S*Me*$_2$ signal for Pd-coordinated dmso ($\delta_{dmso\text{-}Pd}$ ~2.95 ppm). To this solution an additional ligand *L* was added and a $^1$H-NMR spectra was recorded for determination of the new upfield shifted O=S*Me*$_2$ signal ($\delta_{eq}$). The ratio of added ligand was determined by integration. For comparison the shift of uncoordinated dmso was determined from a 1.6 x $10^{-2}$ M solution of dmso in $CD_2Cl_2$ ($\delta_{dmso}$ ~ 2.54 ppm). From the NMR-shifts the ratio of the ligand-substituted complex ($\chi_{Pd\text{-}L}$) was calculated according to equation 1.

$$\chi_{Pd-L} = \frac{\delta_{eq} - \delta_{dmso-Pd}}{\delta_{dmso} - \delta_{dmso-Pd}} \qquad \text{(eq. 1)}$$

The equilibrium constant $K_L$ could then be calculated according to equation 2:

$$K_L = \frac{[Pd-L][dmso]}{[Pd-dmso][L]}$$

$$\Rightarrow \quad K_L = \frac{\{\chi_{Pd-L}[Pd-dmso]_0\}^2}{\{(1-\chi_{Pd-L})[Pd-dmso]_0\}\{[L]_0 - \chi_{Pd-L}[Pd-dmso]_0\}} \qquad \text{(eq. 2)}$$

Note that the main error of this method arises from shift determination, since resonances are broad. Most accurate results are obtained if the new dmso shift is situated rather in the middle of the range between coordinated and free dmso. Hence, for different $K_L$ different amounts of the ligand *L* have do be added for comparable errors.

**Table S1.** Determination of $K_L$ for different ligands.

| Entry | Ligand | $[1\text{-dmso}]_0$[a] | equiv. L | $\delta_{dmso\text{-}Pd}$ [ppm] | $\delta_{dmso}$ [ppm] | $\delta_{eq}$ [ppm] | K |
|---|---|---|---|---|---|---|---|
| S1-1 | $OPPh_3$ | 1.6 | 9.2 | 2.95 | 2.54 | 2.67 | 0.2 |
| S1-2 | $OPBu_3$ | 1.6 | 1.0 | 2.95 | 2.54 | 2.68 | 3.5 |
| S1-3 | $OPOct_3$ | 1.6 | 1.2 | 2.95 | 2.54 | 2.66 | 3.3 |
| S1-4 | $OP(p\text{-}CF_3C_6H_4)_3$ | 1.6 | 10.2 | 2.95 | 2.54 | 2.77 | 0.04 |
| S1-5 | $OP(3,5\text{-}(CF_3)_2C_6H_3)$ | 0.8[b] | 9.2 | 2.95 | 2.54 | 2.91[b] | 0.001[b] |
| S1-6 | $OP(2\text{-}MeC_6H_4)_3$ | 1.6 | 11.3 | 2.95 | 2.54 | 2.78 | 0.03 |
| S1-7 | MeOH | 1.5 | 9.4 | 2.95 | 2.54 | 2.82 | 0.02 |
| S1-8 | 2,6-lutidine | 1.6 | 1.4 | 2.95 | 2.54 | 2.54[c] | $>>10^2$ |
| S1-9 | $MeSO_3C_6H_5$ | 1.6 | 38 | 2.94 | 2.54 | 2.93[d] | $<<10^{-4}$ |

[a]$[10^{-2}$ molL$^{-1}]$, [b]experiment limited due to low solubility of $OPR_3$ in $CD_2Cl_2$, K-value represents rather a rough approximation. [c]2,6-lutidine displaces dmso at any concentration (equiv <<1) completely. [d]Methyl benzenesulfonate does not displace dmso under standard conditions.

**Temperature dependence of $K_L$**

To investigate the influence of the temperature on the coordination equilibrium, $K_{OPPh3}$ was determined in the temperature range between -25 °C and 25 °C. Therefore all shifts were determined at each temperature separately (Table S2). Plotting the natural logarithm of the equilibrium constants against the temperature (Van't Hoff plot) gave values for the reaction enthalpy $\Delta H° = 8$ kJ mol$^{-1}$ and entropy $\Delta S° = 13$ J mol$^{-1}$K$^{-1}$ and evidenced a low temperature dependence (Figure S1). Extrapolation to 90 °C and -80 °C gave $K_{90\,°C} = 0.4$ and $K_{-80\,°C} = 0.04$ respectively.

**Table S2.** Determination of $K_{OPPh3}$ at different temperatures.

| Entry | Ligand | T [°C] | $[1\text{-dmso}]_0$[a] | equiv. L | $\delta_{dmso\text{-}Pd}$ [ppm] | $\delta_{dmso}$ [ppm] | $\delta_{eq}$ [ppm] | K x $10^{-1}$ |
|---|---|---|---|---|---|---|---|---|
| S2-1 | $OPPh_3$ | 25.5 | 1.6 | 10.3 | 2.951 | 2.558 | 2.658 | 2.3 |
| S2-2 | $OPPh_3$ | 14.5 | 1.6 | 10.3 | 2.957 | 2.550 | 2.666 | 1.9 |
| S2-3 | $OPPh_3$ | 6.0 | 1.6 | 10.3 | 2.966 | 2.548 | 2.672 | 1.7 |
| S2-4 | $OPPh_3$ | -4.5 | 1.6 | 10.3 | 2.974 | 2.549 | 2.681 | 1.6 |
| S2-5 | $OPPh_3$ | -15.0 | 1.6 | 10.3 | 2.980 | 2.549 | 2.692 | 1.4 |
| S2-6 | $OPPh_3$ | -25.0 | 1.6 | 10.3 | 2.982 | 2.545 | 2.703 | 1.2 |

[a]$[10^{-2}$ molL$^{-1}]$.

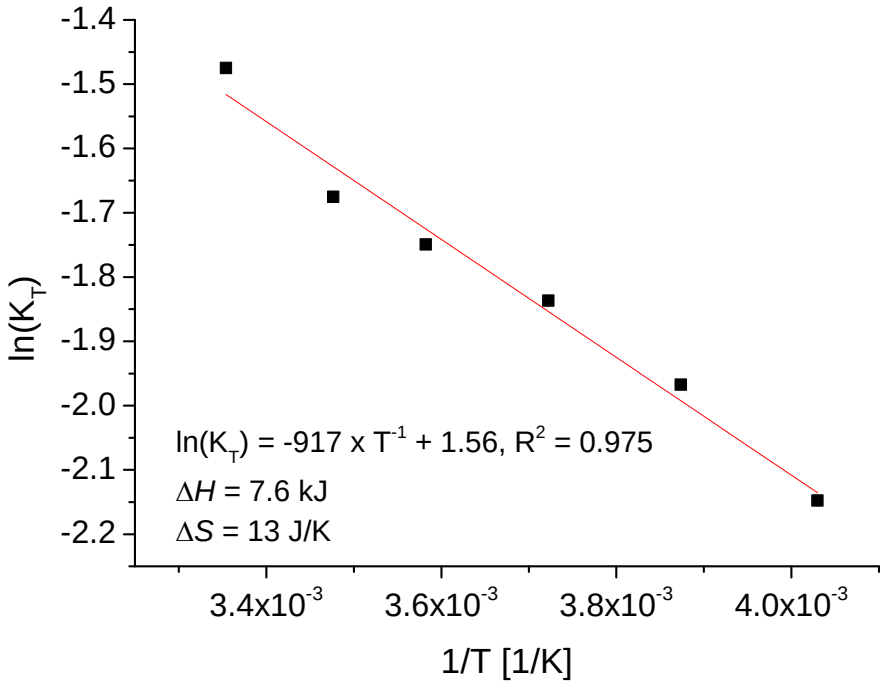


**Figure S1.** Van't Hoff plot for the equilibrium **1-dmso** + $OPPh_3$ ⇆ **1-$OPPh_3$** + dmso determined by variable temperature $^1$H-NMR spectroscopy from T = -25 °C to 25 °C.

## IV. Stability of [(P^O)PdMe(L)] Complexes with Weak Coordinating Ligands

Equilibrium studies have shown that for the investigated phosphine oxides coordination strengths vary between 3.5 to 0.001 in comparison to dmso. Therefore synthesis of the corresponding Pd complexes for polymerization studies was attempted. Synthesis of **1–OPBu$_3$**, **1-OPOct$_3$,** and **1-OPPh$_3$** is described in experimental details section. Consequently interaction of the phosphine oxide with the Pd-centre can be shown by $^{31}$P-NMR in solution (Figure S2) and by ATR-IR in the solid state (Figure S3, S7).[7] For the weaker coordinating OPTol$_3$ and OP(*p*-$CF_3C_6H_4)_3$ a Pd-OPR$_3$ interaction is also visible for the solid raw material (Figure S4). Dissolving the isolated material in $CH_2Cl_2$ yields a clear solution and the $^{31}$P-NMR spectra of the dissolved raw material shows a further reduced but significant shift for the OPR$_3$ signal ($\Delta\delta$ = 3-4 ppm, Figure S4, S5). However, with time a white precipitate is formed, which could be identified as **1$_n$** by NMR, IR, and CHN-analysis (Figure 3, S8, S10). Furthermore it could be shown that OP(*p*-$CF_3C_6H_4)_3$ can be extracted from the complex by simple washing with pentane by which **1–OP(*p*-$CF_3C_6H_4)_3$** is transformed to **1$_n$** (Figure S7). In the case of the significantly weaker coordinating OP(3,5-$(CF_3)_2C_6H_3)_3$ crude **1-OP(3,5-$(CF_3)_2C_6H_3)_3$** already contains substantial amounts of **1$_n$** as evidenced by the IR spectrum, the limited solubility and the ratio of anisyl-methoxy to aromatic 3,5-$(CF_3)_2C_6H_4$-signals detected by $^1$H-NMR (Figure S8, S9).

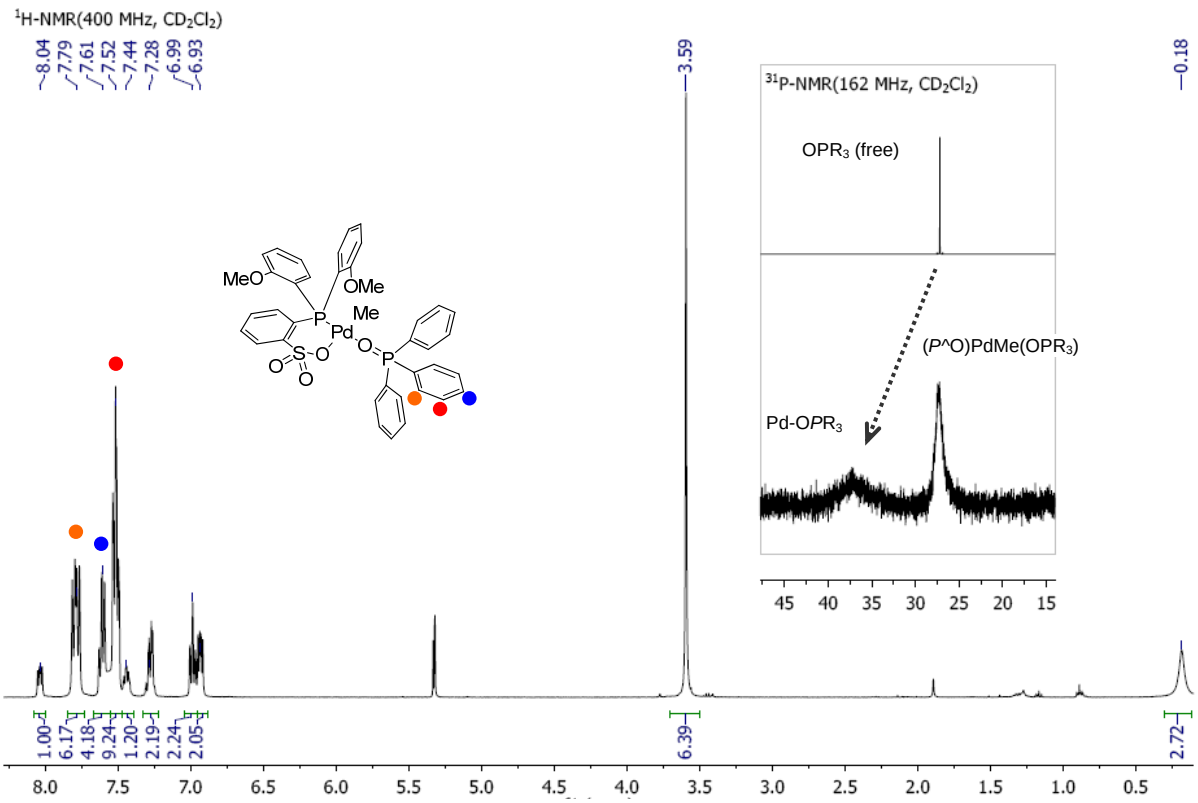


**Figure S2.** $^{1}$H-NMR spectrum (400 MHz, $CD_2Cl_2$) of **1-OPPh$_3$**; Inset: $^{31}$P-NMR (162 MHz, $CD_2Cl_2$) spectra of **1-OPPh$_3$** and $OPPh_3$.

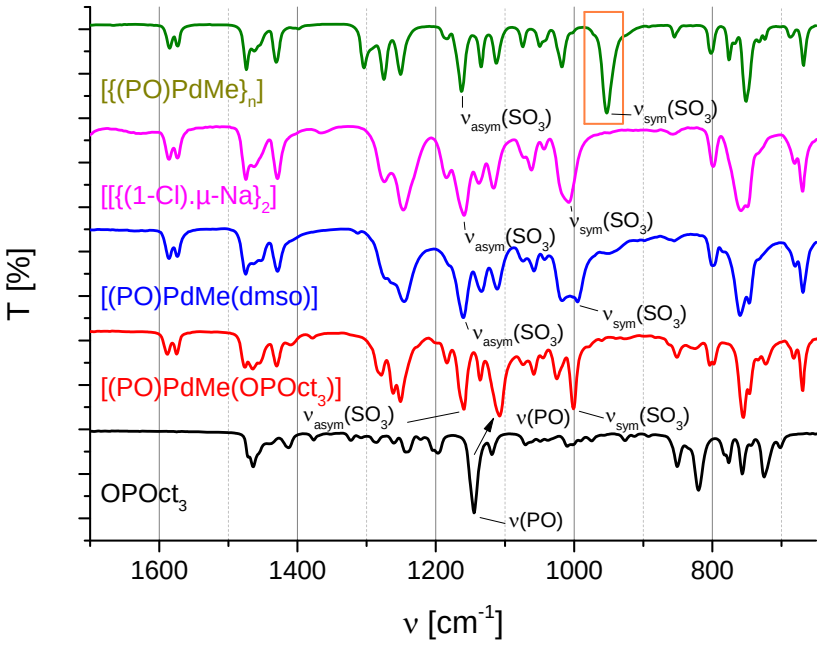


**Figure S3.** ATR-IR spectra of $OPOct_3$, complexes [(P^O)PdMe(L)] (L = $OPOct_3$, dmso, Cl), and the ligand free complex $\mathbf{1_n}$

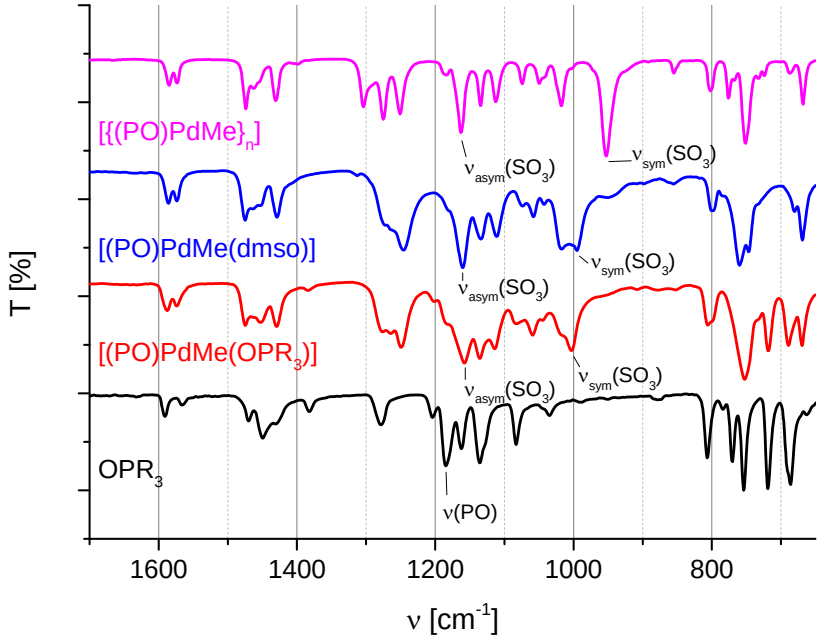


**Figure S4.** ATR-IR spectra of OP(*o*-Tol)$_3$, complexes [(P^O)PdMe(L)] (L = OP(2-Me$C_6H_4$)$_3$, dmso), and the ligand free complex $\mathbf{1_n}$.

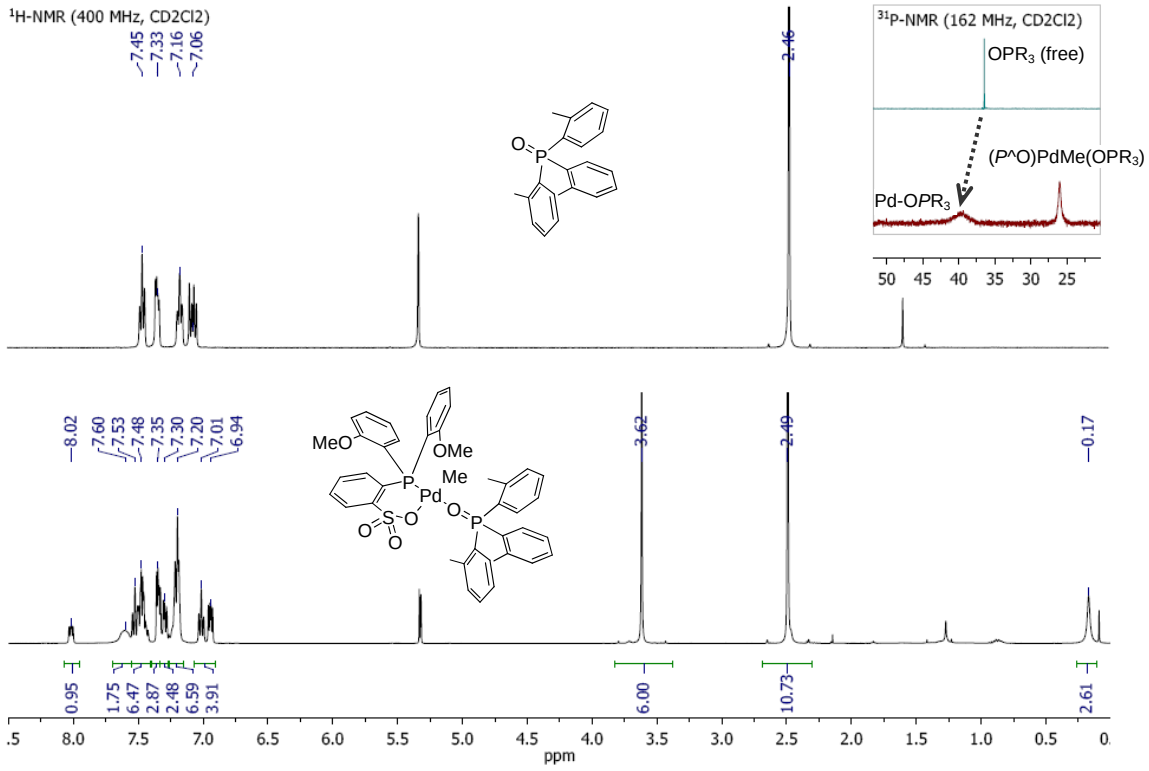


**Figure S5.** $^{1}$H-NMR spectra (400 MHz, $CD_2Cl_2$) of OP(*o*-Tol)$_3$ and **1-OP(*o*-Tol)$_3$** before work up; Inset: $^{31}$P-NMR (162 MHz, $CD_2Cl_2$) spectra.

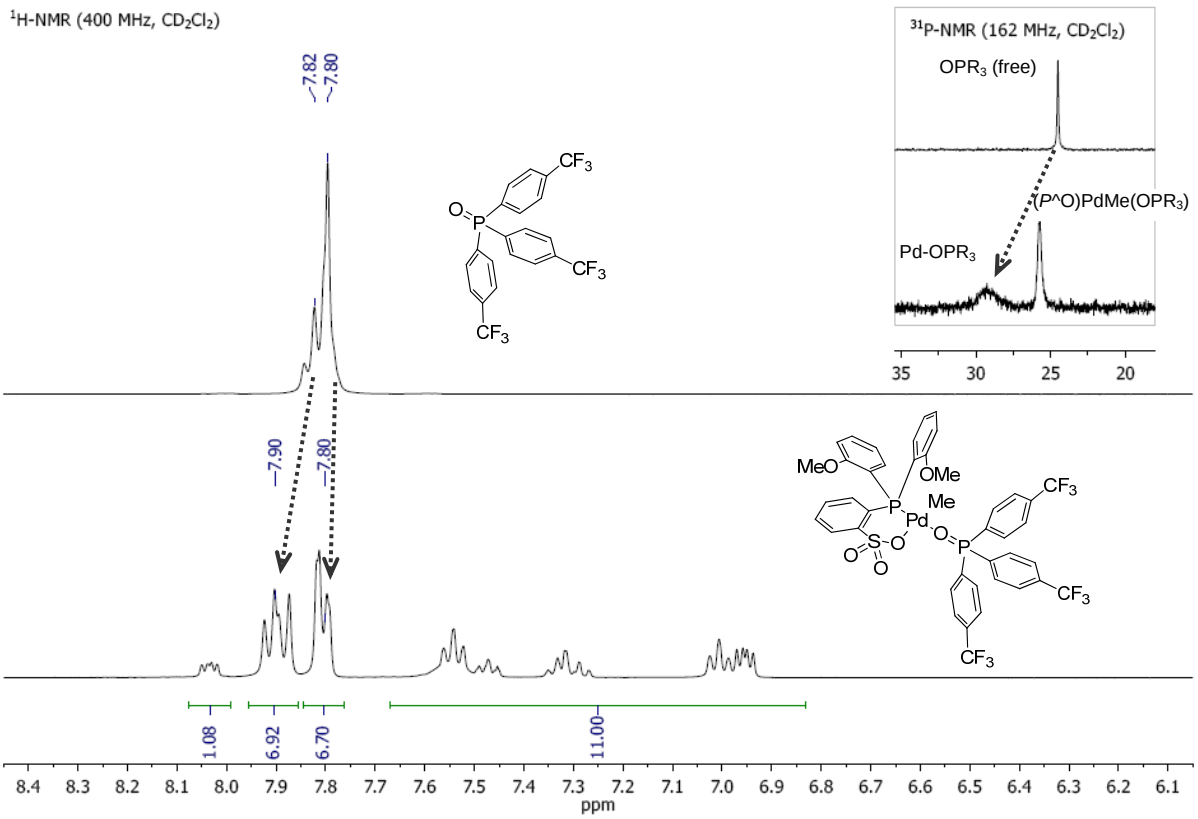


**Figure S6.** $^{1}$H-NMR spectra (400 MHz, $CD_2Cl_2$) of OP($p$-$CF_3C_6H_4$)$_3$ and **1-OP($p$-$CF_3C_6H_4$)$_3$** before work up; Inset: $^{31}$P-NMR (162 MHz, $CD_2Cl_2$) spectra.

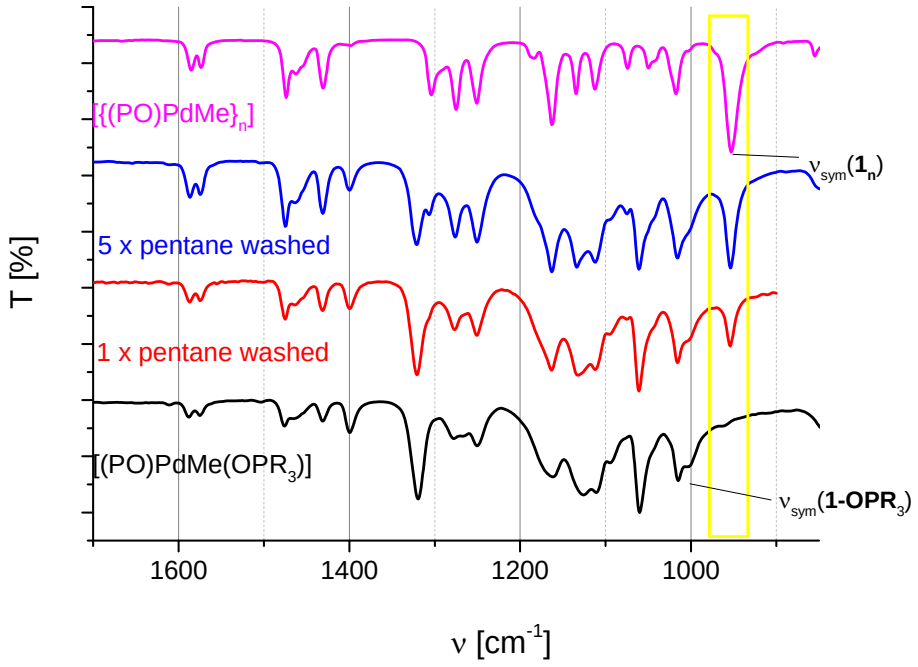


**Figure S7.** ATR-IR spectra of **1- OP(*p*-$CF_3C_6H_4)_3$** and transformation into the ligand free complex $\mathbf{1_n}$ by washing crude **1- OP(*p*-$CF_3C_6H_4)_3$** with pentane.

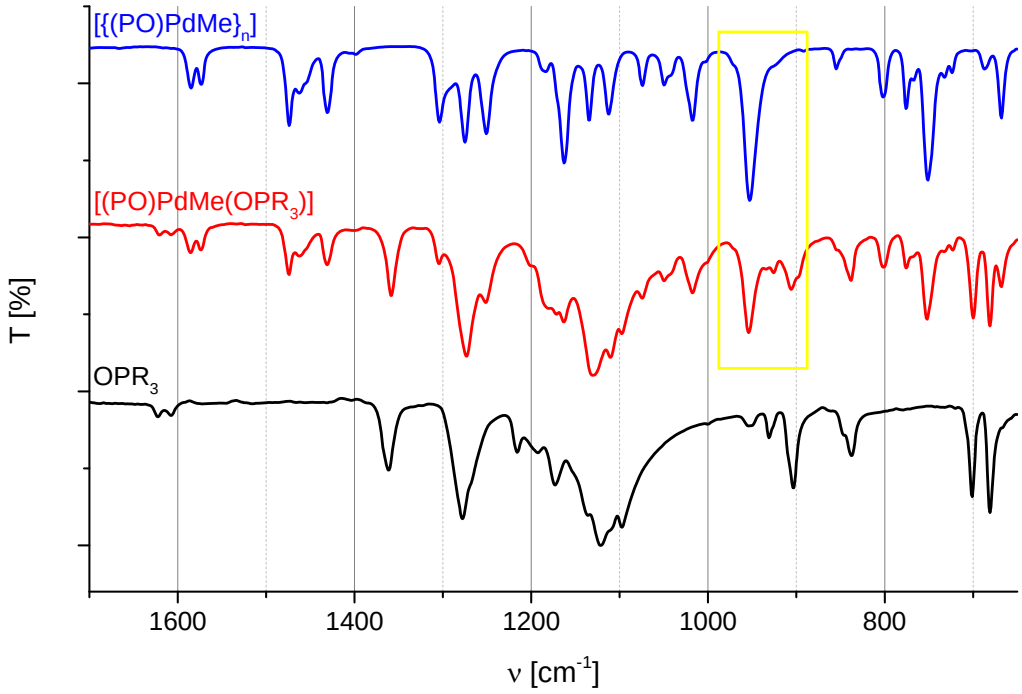


**Figure S8.** ATR-IR spectra of crude **1-OP(3,5-$(CF_3)_2C_6H_3)_3$** in comparison to free OP(3,5-$CF_3(C_6H_3))_3$ and the ligand free complex $\mathbf{1_n}$.

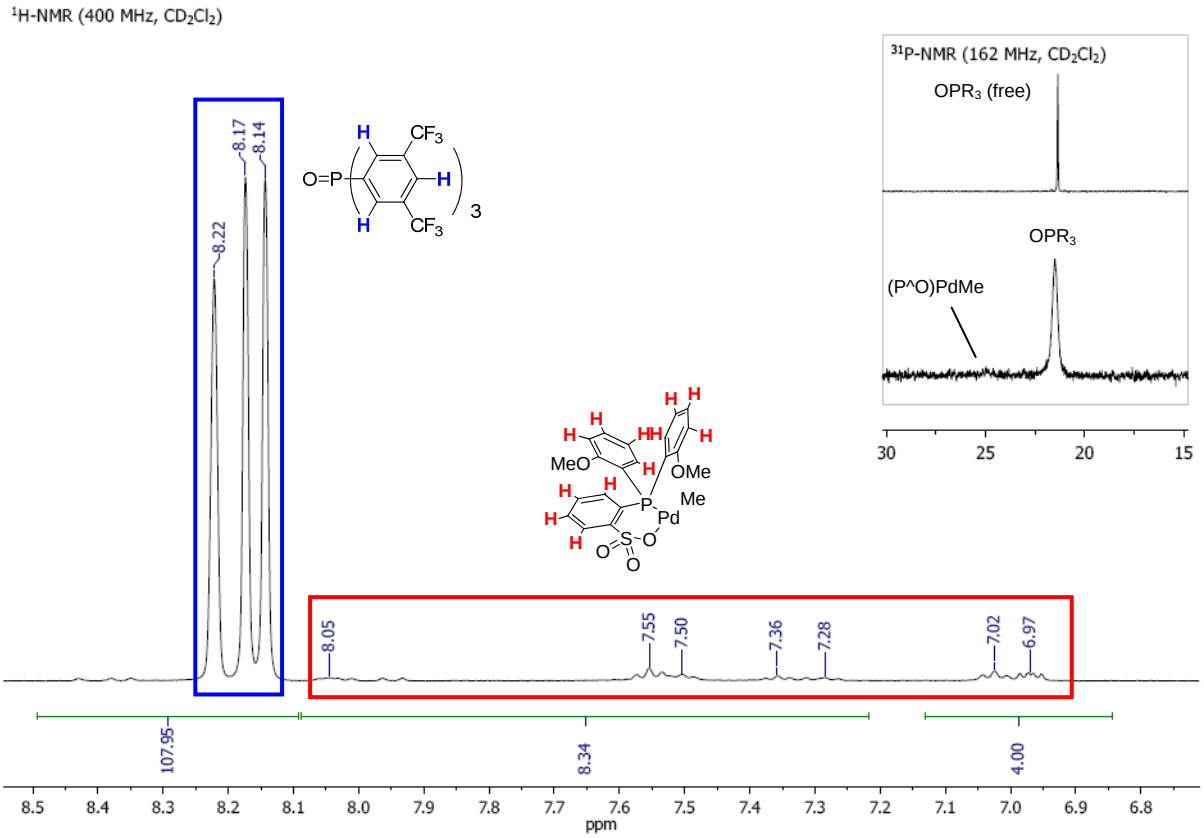


**Figure S9.** $^{1}$H-NMR spectrum (400 MHz, $CD_2Cl_2$) of the reaction of [{(**1-Cl**)-μ-Na}$_2$] with $AgBF_4$ in the presence of OP(3,5-$CF_3(C_6H_3)$)$_3$; Inset: $^{31}$P-NMR (162 MHz, $CD_2Cl_2$) spectra of free phosphine oxide and reaction mixture.

## Analysis of formed precipitates

The formed precipitates were analyzed by means of IR-spectroscopy (*vide supra*) and $^{1}$H-NMR spectroscopy (Figure S10). The spectra are in full accordance with the corresponding spectra of independently synthesized **1$_n$**. Thereby **1$_n$** was synthesized by chloride abstraction from [{(**1-Cl**)-μ-Na}$_2$] with $AgBF_4$ in $CH_2Cl_2$. The reaction mixture was evaporated and the residue was washed with $CH_2Cl_2$ to yield **1$_n$**. The identity of **1$_n$** could unambiguously be confirmed by comparison to literature[8,9] and by CHN-analysis: **Anal. Calcd.** (%) for **1$_n$** ([$C_{21}H_{21}O_5PPdS$]$_n$): C, 48.24; H, 4.05; Found: C, 48.07; H, 4.00.

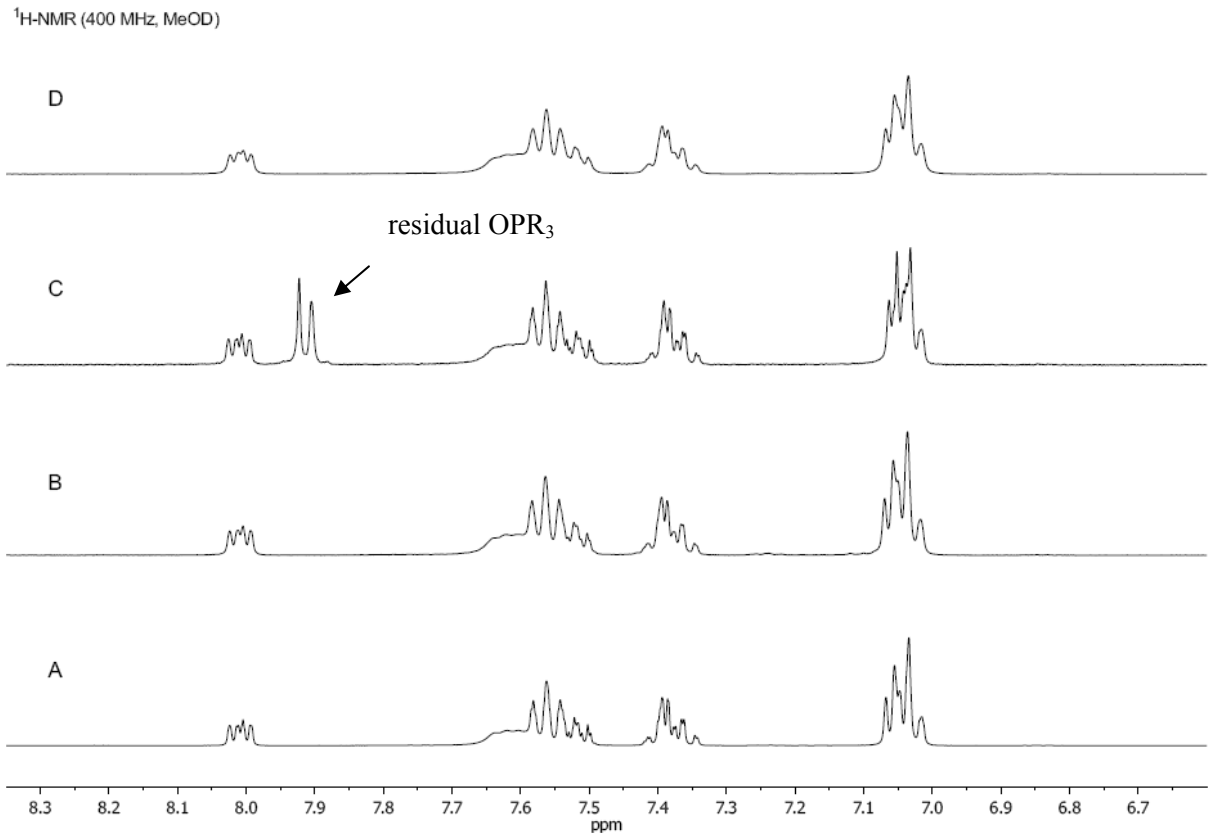


**Figure S10.** $^1$H-NMR spectra (400 MHz, MeOD) of $[(P\text{^}O)PdMe]_n$ (A) and the separated precipitates from solutions of [(P^O)PdMe(L)] (L = OP(*o*-Tol)$_3$ (B), OP(*p*-$CF_3C_6H_4$)$_3$ (C), OP(3,5-$(CF_3)_2C_6H_3$)$_3$ (D)) in $CD_2Cl_2$.

**Isolation and decomposition of 1-MeOH**

Kinetic effects can be dominant for unexpected stabilization of [(P^O)PdMe(L)] complexes. This is demonstrated by the isolation of **1-MeOH** by crystallization from a solution of $\mathbf{1_n}$ in MeOH and characterization by X-Ray analysis (Figure S14). Methanol binds less strongly to (P^O)PdMe than OP(*o*-Tol)$_3$ or OP(*p*-$CF_3C_6H_4$)$_3$ for which no stable complexes could be isolated (*vide supra*, $K_{MeOH}$ = 0.02 vs $K_{OP(o\text{-Tol})3}$ = 0.03, $K_{OP(p\text{-CF3Ar})3}$ = 0.04). The instability of **1-MeOH** can impressively be demonstrated by the transformation to $\mathbf{1_n}$ at the air in the solid state: Single crystals of **1-MeOH** freshly prepared from a solution of $\mathbf{1_n}$ in MeOH were transferred to the surface of the ATR-IR unit of the IR-spectrometer, while the crystals still were slightly wetted with MeOH. The transformation of **1-**

**MeOH** to $\mathbf{1_n}$ was monitored by IR-spectroscopy and was found to be completed within 20 minutes (Figure S11).

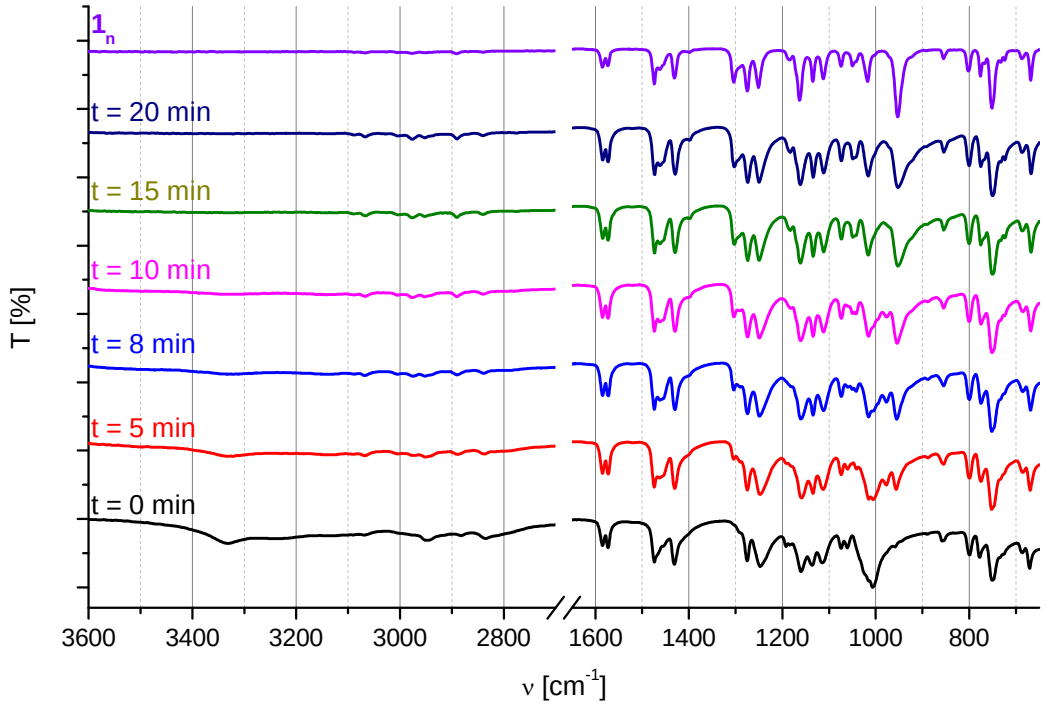


**Figure S11.** ATR-IR spectra of the transformation of **1-MeOH** to $\mathbf{1_n}$ with time at the air.

## V. Single Crystal X-Ray Diffraction

X-Ray diffraction analyses were performed at 100 K on a STOE IPDS-II diffractometer equipped with a graphite monochromated radiation source (Mo-$K_\alpha$, $\lambda$ = 0.71073 Å) and an image plate detection system. Crystals were mounted on a fine glass fibre with silicon grease. The selection, integration, and averaging procedure of the measured reflex intensities, the determination of the unit cell dimensions and a least-squares fit of the 2$\theta$ values as well as data reduction, LP-correction and space group determination were performed using the X-Area software package delivered with the diffractometer.[10] A semiempirical absorption correction was performed. The structures were solved by the Patterson and direct methods (SHELXS-97)[11], completed with difference fourier syntheses, and refined with full-matrix least-square using SHELXL-97[12] minimizing $\omega(F_0^2 - F_c^2)^2$ . Weighted *R* factor ($wR_2$) and the goodness of fit GooF are based on $F^2$. All non-hydrogen atoms were refined with anisotropic displacement parameters. All hydrogen atoms except the hydroxyl proton of the coordinated MeOH molecule (H24) in **1-MeOH** were treated in a riding model. Structures were plotted using Diamond 3.1.[13] The drawn ellipsoids represent 50% probability.

**Table S3.** Crystallographic Data of Complex **1-OPBu$_3$**

| | |
|---|---|
| **CCDC deposit no** | **862044** |
| Crystal description | colourless fragment |
| Formula | C33 H48 O6 P2 Pd S |
| Formula weight | 741.11 |
| Crystal Size [mm$^3$] | 0.50 x 0.28 x 0.05 |
| Crystal System | Triclinic |
| Space group | $P_{-1}$ (2) |
| a [Å] | 12.0993(8) |
| b [Å] | 12.0348(8) |
| c [Å] | 13.4363(8) |
| α [°] | 77.079(5) |
| β [°] | 69.231(5) |
| γ [°] | 75.256(5) |
| V [Å$^3$] | 1749.78(19) |
| Z | 2 |
| $\rho_{calc}$ [g·cm-3] | 1.407 |
| μ (Mo-Kα) [mm$^{-1}$] | 0.722 |
| F(000) | 772 |
| T [K] | 100 |
| Wavelenght [Å] | 0.71073 (Mo-K$_\alpha$) |
| Diffractometer | STOE IPDS 2T |
| Scan | ω-scan |
| θmin-max [°] | 1.77-27.94 |
| (sinθ/λ)max [Å$^{-1}$] | 0.63 |
| Data total / unique | 28093/8347 |
| $R_{int}$ | 0.0914 |
| $R_{sigma}$ | 0.0752 |
| Data obs ($F^2 \geq 4\sigma(F^2)$) | 6679 |
| hkl-range | -15/15, -15/15, -17/17 |
| Absorption correction | numerical Integration |
| Structure Solution | SHELXS-97[11] |
| Structure Refinement | SHELXL-97[12] |
| H atoms | constrained |
| Number Parameters | 397 |
| R(F) obs. / all | 0.0394/ 0.0581 |
| wR($F^2$) all | 0.0811 |
| w (a, b)[a] | 0.0344, 0.000 |
| GoF ($F^2$) | 0.986 |
| $dU_{max}$ | 0.000 |
| $\Delta\rho_{fin}$ (min./max.) [e·Å$^{-3}$] | 0.679/-1.004 |

[a] weighting scheme: $w = 1/[\sigma^2(Fo^2) + (a \cdot P)^2 + b \cdot P)$, $P = [\max(Fo^2,0) + 2\,Fc^2]/3$.

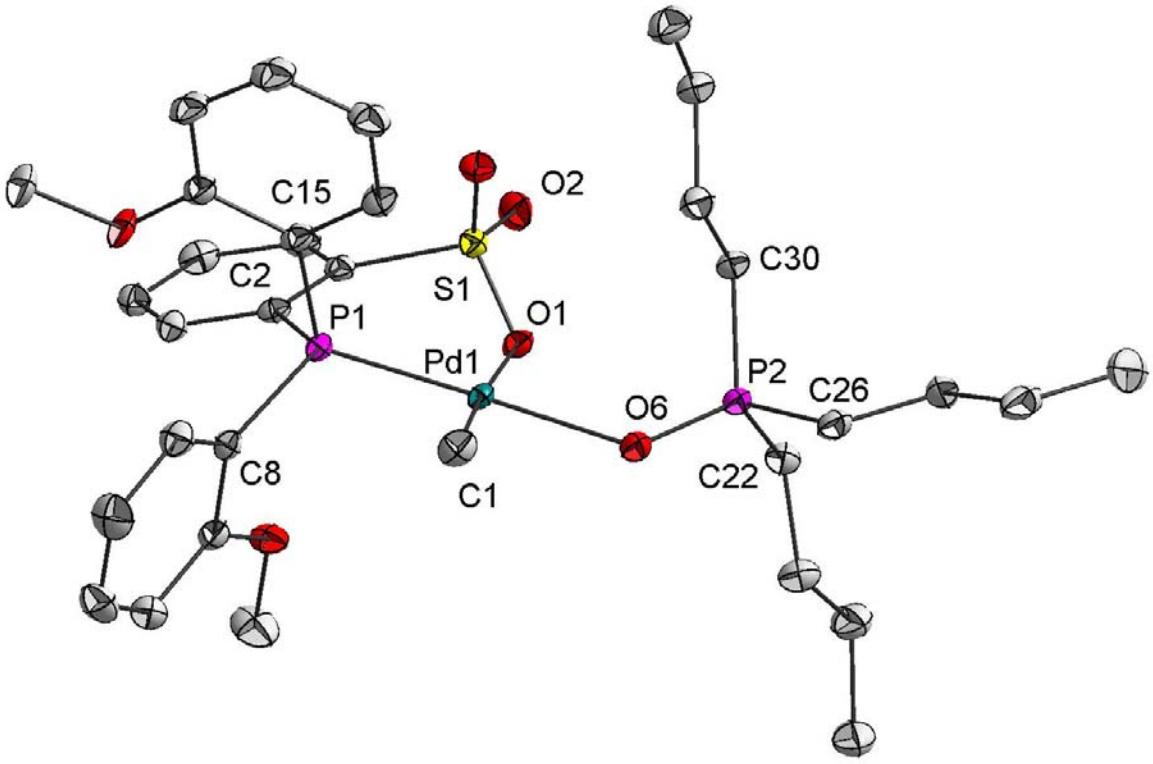


**Figure S12.** Solid state structure of **1-OPBu$_3$**. Ellipsoids represent 50% probability. Hydrogen atoms have been omitted for clarity.

**Table S4.** Selected bond length [Å] and angles [°] for **1-OPBu$_3$**.

| | | | |
|---|---|---|---|
| Pd-P1 | 2.203(1) | P2-C26 | 1.803(3) |
| Pd-C1 | 2.010(3) | O1-S1 | 1.491(2) |
| Pd-O1 | 2.157(2) | S1-O2 | 1.444(2) |
| Pd-O6 | 2.129(2) | P1-C15 | 1.819(3) |
| O6-P2 | 1.514(2) | P1-C2 | 1.839(3) |
| | | | |
| P1-Pd-O1 | 96.1(1) | P1-Pd-C1 | 88.1(1) |
| C1-Pd-O6 | 86.3(1) | O1-Pd-O6 | 89.5(1) |
| O6-P2-C22 | 112.1(1) | C22-P2-C26 | 106.6(1) |
| Pd-O6-P2 | 132.1(1) | P1-Pd-O6 | 174.4(1) |

**Table S5.** Crystallographic Data of Complex **1-OPPh$_3$**

| **CCDC deposit no** | **862045** |
|---|---|
| Crystal description | colourless cube |
| Formula | C39 H36 O6 P2 Pd S * C H Cl3 |
| Formula weight | 920.45 |
| Crystal Size [mm$^3$] | 0.20 x 0.20 x 0.20 |
| Crystal System | Monoclinic |
| Space group | P21/c (14) |
| a [Å] | 14.2186(5) |
| b [Å] | 10.6220(5) |
| c [Å] | 29.5485(12) |
| α [°] | 90 |
| β [°] | 115.328(3) |
| γ [°] | 90 |
| V [Å$^3$] | 4033.7(3) |
| Z | 4 |
| $\rho_{calc}$ [g·cm-3] | 1.516 |
| μ (Mo-Kα) [mm$^{-1}$] | 0.711 |
| F(000) | 1872 |
| T [K] | 100(2) |
| Wavelenght [Å] | 0.71073 (Mo-K$_\alpha$) |
| Diffractometer | STOE IPDS 2T |
| Scan | ω-scan |
| θmin-max [°] | 2.06-26.87 |
| (sinθ/λ)max [Å$^{-1}$] | 0.67 |
| Data total / unique | 56509/8624 |
| $R_{int}$ | 0.0784 |
| $R_{sigma}$ | 0.0432 |
| Data obs ($F^2 \geq 4\sigma(F^2)$) | 6928 |
| hkl-range | -17/18, -13/13, -37/37 |
| Absorption correction | numerical Integration |
| Structure Solution | SHELXS-97[11] |
| Structure Refinement | SHELXL-97[12] |
| H atoms | constrained |
| Number Parameters | 481 |
| R(F) obs. / all | 0.0459/ 0.0647 |
| wR($F^2$) all | 0.1036 |
| w (a, b)[a] | 0.043, 9.46 |
| GoF ($F^2$) | 1.033 |
| $dU_{max}$ | 0.000 |
| $\Delta\rho_{fin}$ (min./max.) [e·Å$^{-3}$] | 2.750/-1.678 |

[a] weighting scheme: $w = 1/[\sigma^2(Fo^2) + (a\cdot P)^2 + b\cdot P)$, $P = [\max(Fo^2,0) + 2\,Fc^2]/3$.

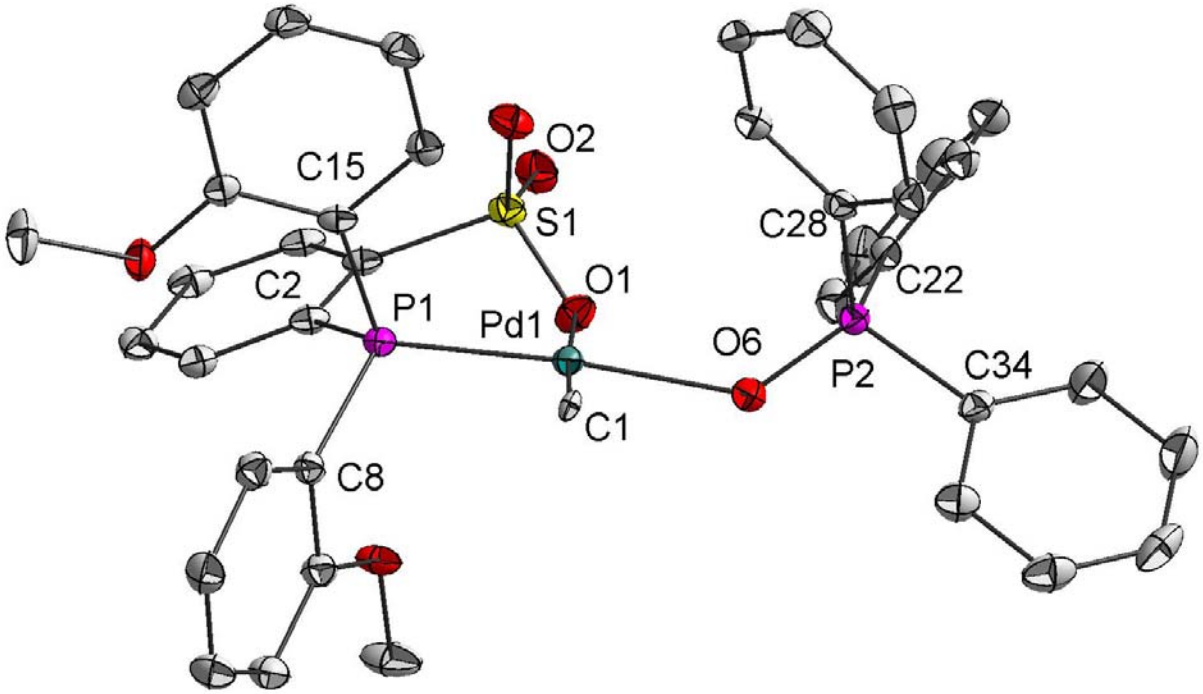


**Figure S13.** Solid state structure of **1-OPPh$_3$**. Ellipsoids represent 50% probability. Hydrogen atoms and solvent molecules have been omitted for clarity.

**Table S6.** Selected bond length [Å] and angles [°] for **1-OPPh$_3$**.

| | | | |
|---|---|---|---|
| Pd-P1 | 2.199(1) | P2-C34 | 1.804(5) |
| Pd-C1 | 2.089(3) | O1-S1 | 1.485(3) |
| Pd-O1 | 2.150(3) | S1-O2 | 1.450(3) |
| Pd-O6 | 2.138(3) | P1-C15 | 1.815(4) |
| O6-P2 | 1.503(3) | P1-C2 | 1.837(4) |
| | | | |
| P1-Pd-O1 | 94.9(1) | P1-Pd-C1 | 88.0(1) |
| C1-Pd-O6 | 89.7(1) | O1-Pd-O6 | 87.5(1) |
| O6-P2-C34 | 109.0(2) | C22-P2-C34 | 107.5(2) |
| Pd-O6-P2 | 133.5(1) | P1-Pd-O6 | 175.2(1) |

**Table S7.** Crystallographic Data of Complex **1-MeOH**

| | |
|---|---|
| **CCDC deposit no** | **862043** |
| Crystal description | colourless cube |
| Formula | C22 H25 O6 P Pd S * C H4 O |
| Formula weight | 586.89 |
| Crystal Size [$mm^3$] | 0.50 x 0.38 x 0.25 |
| Crystal System | Monoclinic |
| Space group | P21/c (14) |
| a [Å] | 11.4001(6) |
| b [Å] | 14.0634(6) |
| c [Å] | 15.5159(9) |
| α [°] | 90 |
| β [°] | 93.681(5) |
| γ [°] | 90 |
| V [$Å^3$] | 2482.4(2) |
| Z | 4 |
| $\rho_{calc}$ [$g \cdot cm^{-3}$] | 1.570 |
| μ (Mo-Kα) [$mm^{-1}$] | 0.937 |
| F(000) | 1200 |
| T [K] | 100(2) |
| Wavelenght [Å] | 0.71073 (Mo-$K_\alpha$) |
| Diffractometer | STOE IPDS 2T |
| Scan | ω-scan |
| θmin-max [°] | 1.79-28.69 |
| (sinθ/λ)max [$Å^{-1}$] | 0.65 |
| Data total / unique | 43129/6310 |
| $R_{int}$ | 0.0466 |
| $R_{sigma}$ | 0.027 |
| Data obs ($F^2 \geq 4\sigma(F^2)$) | 5598 |
| hkl-range | -15/15, -18/18, -20/50 |
| Absorption correction | numerical Integration |
| Structure Solution | SHELXS-97[11] |
| Structure Refinement | SHELXL-97[12] |
| H atoms | constrained |
| Number Parameters | 313 |
| R(F) obs. / all | 0.0270/ 0.0346 |
| wR($F^2$) all | 0.0594 |
| w (a, b)[a] | 0.0221, 2.8492 |
| GoF ($F^2$) | 1.046 |
| $dU_{max}$ | 0.000 |
| $\Delta\rho_{fin}$ (min./max.) [$e \cdot Å^{-3}$] | 0.446/-0.943 |

[a] weighting scheme: $w = 1/[\sigma^2(Fo^2) + (a \cdot P)^2 + b \cdot P)$, $P = [max(Fo^2,0) + 2\ Fc^2]/3$.

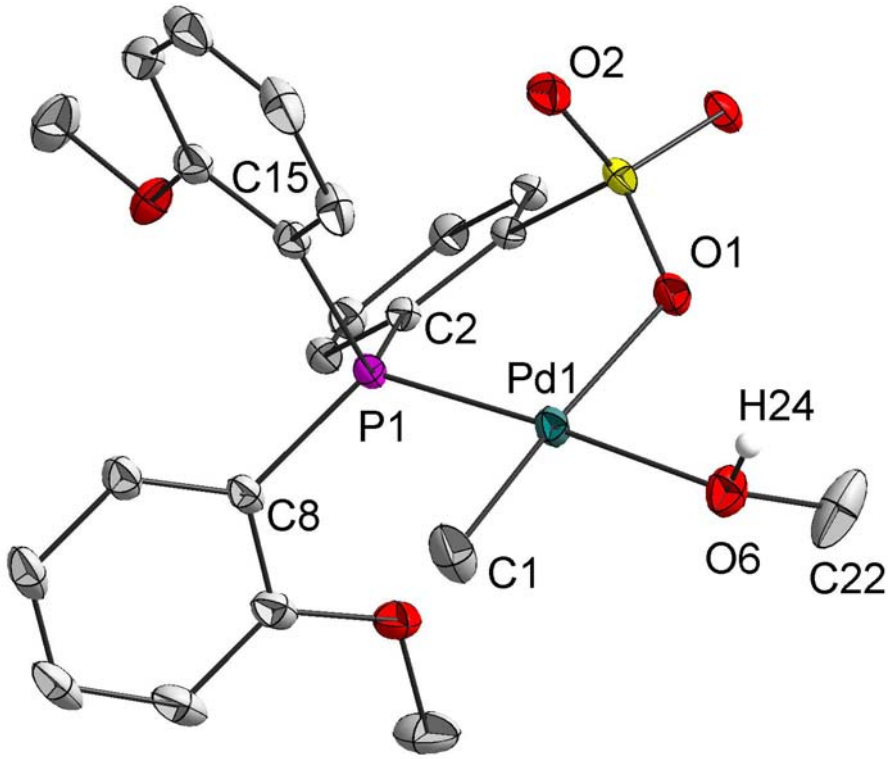


**Figure S14.** Solid state structure of **1-MeOH**. Ellipsoids represent 50% probability. Hydrogen atoms, except the hydroxyl hydrogen H24, and solvent molecules have been omitted for clarity.

**Table S8.** Selected bond length [Å] and angles [°] for **1-MeOH**.

| | | | |
|---|---|---|---|
| Pd-P1 | 2.200(1) | O1-S1 | 1.478(1) |
| Pd-C1 | 2.032(2) | O2-S1 | 1.440(2) |
| Pd-O1 | 2.158(1) | P1-C15 | 1.812(2) |
| Pd-O6 | 2.139(2) | P1-C2 | 1.836(2) |
| O6-C22 | 1.429(3) | P1-C8 | 1.818(2) |
| | | | |
| P1-Pd-O1 | 95.4(0) | P1-Pd-C1 | 89.5(1) |
| C1-Pd-O6 | 88.4(1) | O1-Pd-O6 | 86.8(1) |
| Pd-O6-C22 | 118.2(1) | P1-Pd-O6 | 176.9(0) |

## VI. Homopolymerization of Ethylene

Polymerizations were carried out in a 250 mL stainless steel mechanically stirred (1000 rpm) pressure reactor equipped with a heating/cooling jacket supplied by a thermostat controlled by a thermocouple dipping into the polymerization mixture. A valve controlled by a pressure transducer allowed for applying and keeping up a constant ethylene pressure. The required flow of ethylene, corresponding to ethylene consumed by polymerization, was monitored by a mass flow meter and recorded digitally. Prior to a polymerization experiment, the reactor was heated under vacuum to the desired reaction temperature for 30 min and then back-filled with argon.

Standard procedure: A stock solution of the catalyst precursor (8 μmol $mL^{-1}$) in methylene chloride was prepared in the glovebox. Solutions of **1** were prepared by reaction of ½ [{(**1-Cl**)-μ-Na}$_2$] with 1 equiv $AgBF_4$ in $CD_2Cl_2$ and filtration. Theses solutions were and kept in the refrigerator of the glovebox (-30°C) and never stored longer than 12 hours. The reactor was vented, in a slight argon stream the solvent was transferred via cannula (100 mL toluene), and 0.5 mL of the precursor solution was inserted by a syringe to the reactor ([Pd] = 40 μmol $L^{-1}$). The reactor was closed and a constant ethylene pressure was applied. After the desired reaction time the reactor was rapidly vented. The polymerization mixture was poured into 200 mL of MeOH. The polymer was isolated by filtration, washed several times with methanol, and dried in vacuo at 50 °C.

**Table S9.** Ethylene homopolymerization.

| Entry | Catalyst precursor | p [bar] | yield [g] | TOF [x$10^4$][a] |
|---|---|---|---|---|
| S9-1 | **1-OPBu$_3$** | 10 | 8.23 | 15 |
| S9-2 | **1-dmso** | 10 | 8.55 | 15 |
| S9-3 | **1-OPPh$_3$** | 10 | 8.36 | 15 |
| S9-4 | **1** (*in situ*) | 10 | 7.03 | 13 |
| S9-5 | **1-OPBu$_3$** | 5 | 5.96 | 11 |
| S9-6 | **1-dmso** | 5 | 7.84 | 14 |
| S9-7 | **1-OPPh$_3$** | 5 | 7.00 | 12 |
| S9-8 | **1** (*in situ*) | 5 | 9.09 | 17 |
| S9-9 | **1-OPBu$_3$** | 3.5 | 4.18 | 8 |
| S9-10 | **1-dmso** | 3.5 | 4.74 | 9 |
| S9-11 | **1-OPPh$_3$** | 3.5 | 5.15 | 9 |
| S9-12 | **1** (*in situ*) | 3.5 | 6.70 | 12 |
| S9-13 | **1-OPBu$_3$** | 2 | 2.64 | 5 |
| S9-14 | **1-dmso** | 2 | 2.44 | 4 |
| S9-15 | **1-OPPh$_3$** | 2 | 3.32 | 6 |
| S9-16 | **1** (*in situ*) | 2 | 2.80 | 5 |

Reaction conditions: 100 mL of toluene; [Pd] = 40 μmol $L^{-1}$; 90 °C, 30 min polymerization time. [a][mol ($C_2H_4$) mol $(Pd)^{-1}$ $h^{-1}$].

**Catalyst stability**

Mass flow traces were recorded to follow catalyst stability. The Mass flow traces were smoothed by using the Savitzky-Golay-algorithm[14] for comparison:

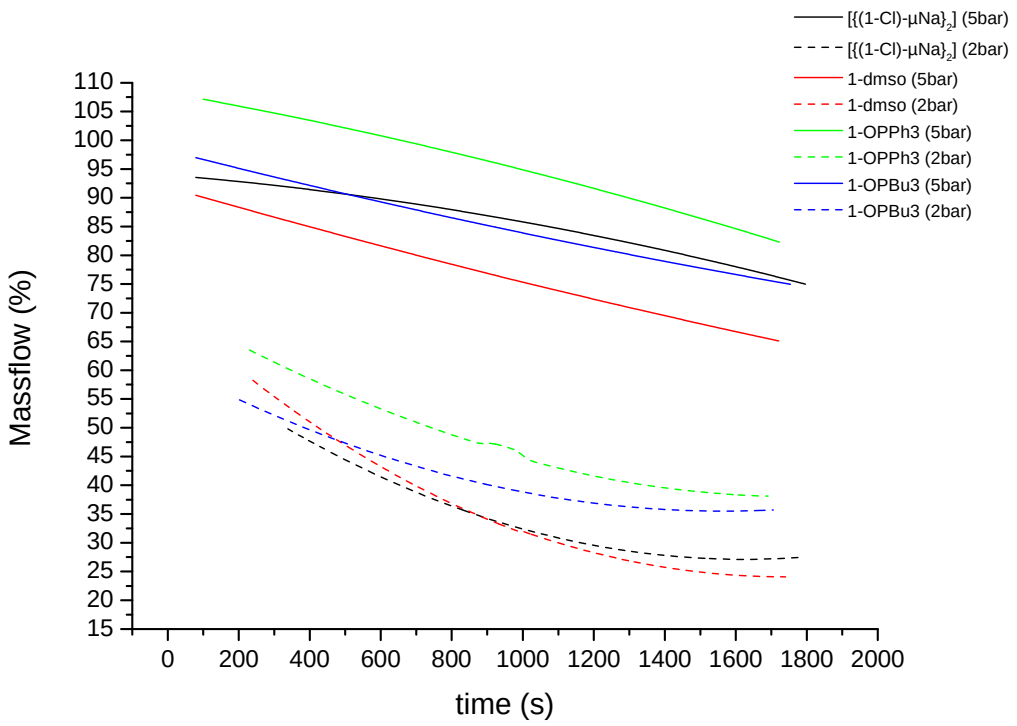


**Figure S15.** Ethylene mass flow versus time for polymerization at 2 bar and 5 bar ethylene pressure.

## VII. Copolymerization of Ethylene and Methyl Acrylate

The copolymerization of ethylene and methyl acrylate was conducted in analogy to ethylene homopolymerizations: A solution of toluene and MA (with a total volume of 50 mL) was cannula transferred into the reactor under an argon counter stream. The catalyst precursor was dissolved in dichloromethane (1 mL) and inserted by a syringe to the reactor. Solutions of **1** were prepared by reaction of ½ [{(**1-Cl**)-μ-Na}$_2$] with 1 equiv $AgBF_4$ in 2 mL $CD_2Cl_2$ and filtration. In order to prevent any radical homopolymerization of methyl acrylate, the radical inhibitor 3,5-di-t-butyl-4-hydroxy-toluene (BHT) was added to the reaction mixture.

In order to prevent loss of any oligomeric material, toluene and comonomer were removed under vacuum and the residue was dried in vacuo at 50 °C for several days.

**Table S10.** Ethylene-methyl acrylate copolymerization

| Entry | Catalyst precursor | yield [g] | $X_{MA}$[a] | $TOF_{C2H4}$[b] | $TOF_{MA}$[c] | $M_n$[a] [$10^3$ g mol$^{-1}$] | $DP_n$[a] | $M_w/M_n$[d] |
|---|---|---|---|---|---|---|---|---|
| S10-1 | **1-OPBu$_3$** | 0.8 | 14.2 | 1927 | 319 | 2.0 | 55 | 1.7 |
| S10-12 | **1-dmso** | 0.9 | 14.8 | 2047 | 356 | 2.3 | 62 | 1.7 |
| S10-13 | **1-OPPh$_3$** | 1.0 | 13.7 | 2404 | 380 | 2.5 | 69 | 1.8 |
| S10-14 | [{(**1-Cl**)-μ-Na}$_2$] | 1.2 | 13.2 | 2888 | 439 | 2.6 | 72 | 1.8 |

Reaction conditions: total volume toluene + MA: 50 mL; [MA] = 0.5 mol L$^{-1}$, 3.5 bar ethylene pressure; 93 °C; 20 μmol Pd(II); 1 h reaction time. [a]Determined by $^1$H NMR in $CDCl_3$ ; [b][mol ($C_2H_4$) mol (Pd)$^{-1}$ h$^{-1}$] ; [c][mol (MA) mol (Pd)$^{-1}$ h$^{-1}$]. [d]determined by GPC.

## VIII. Ethylene Insertion Kinetic

The insertion of ethylene into the Pd-Me bond was monitored by $^1$H-NMR at -15 °C for **1-OPPh$_3$** and *in situ* generated **1** ([{(**1-Cl**)-μ-Na}$_2$] + $AgBF_4$ → **1** + AgCl ↓ + $NaBF_4$↓) under pseudo first order conditions.

General procedure: A J. Young tube containing a solution of 7.2 μmol **1-OPPh$_3$** in $CD_2Cl_2$ (1.3 mM) was pressurized with 0.6 bar ethylene at -80 °C (Pd:$C_2H_4$ = 1:22). At -15 °C the disappearance of the Pd-*Me* signal was monitored by $^1$H-NMR-spectroscopy (Figure S16). While higher palladium-alkyl complexes also insert ethylene, a huge excess of ethylene vs ∑Pd-alkyl (> 10:1) was present during the whole time of the experiment. For kinetic analysis of a ligand free species **1** a solution of 7.2 μmol [{(**1-Cl**)-μ-Na}$_2$] in $CD_2Cl_2$ (0.0013M) was treated with 1.1 equiv $AgBF_4$ in a J. Young tube and shaken for 1 minute, then 0.6 bar ethylene overpressure were applied (Pd:$C_2H_4$ = 1:22).

The pseudo first order plots of the consumption of the Pd-Me signal gave the rate constants $k_{1\text{-OPPh3}}$ = 5.7 × $10^{-4}$ $s^{-1}$ and $k_1$ = 7.0 × $10^{-4}$ $s^{-1}$ respectively (Figure S17). The influence of the weakly coordinating ligand $OPPh_3$ is reflected in the somewhat smaller rate constant $k_{1\text{-OPPh3}}$. The analysis of higher insertions is hampered by the fact that [(P^O)PdR(L)] species precipitate with growing alkyl chain. However, by monitoring the insertion over a period of two hours it becomes obvious that higher insertions into **1** are also significant faster than into **1-OPPh$_3$**, because ethylene is consumed more rapidly. Interestingly, not only ethylene-insertion but also *β*-H elimination is faster with *in situ* generated **1** than with **1-OPPh$_3$** as evidenced by the increasing signal of vinylic end groups of these samples (Figure S18). This is in line with the observation that a solution of the ligand free [(P^O)Pd(polymeryl)] complex in $CD_2Cl_2$ decomposes significantly faster at room temperature.

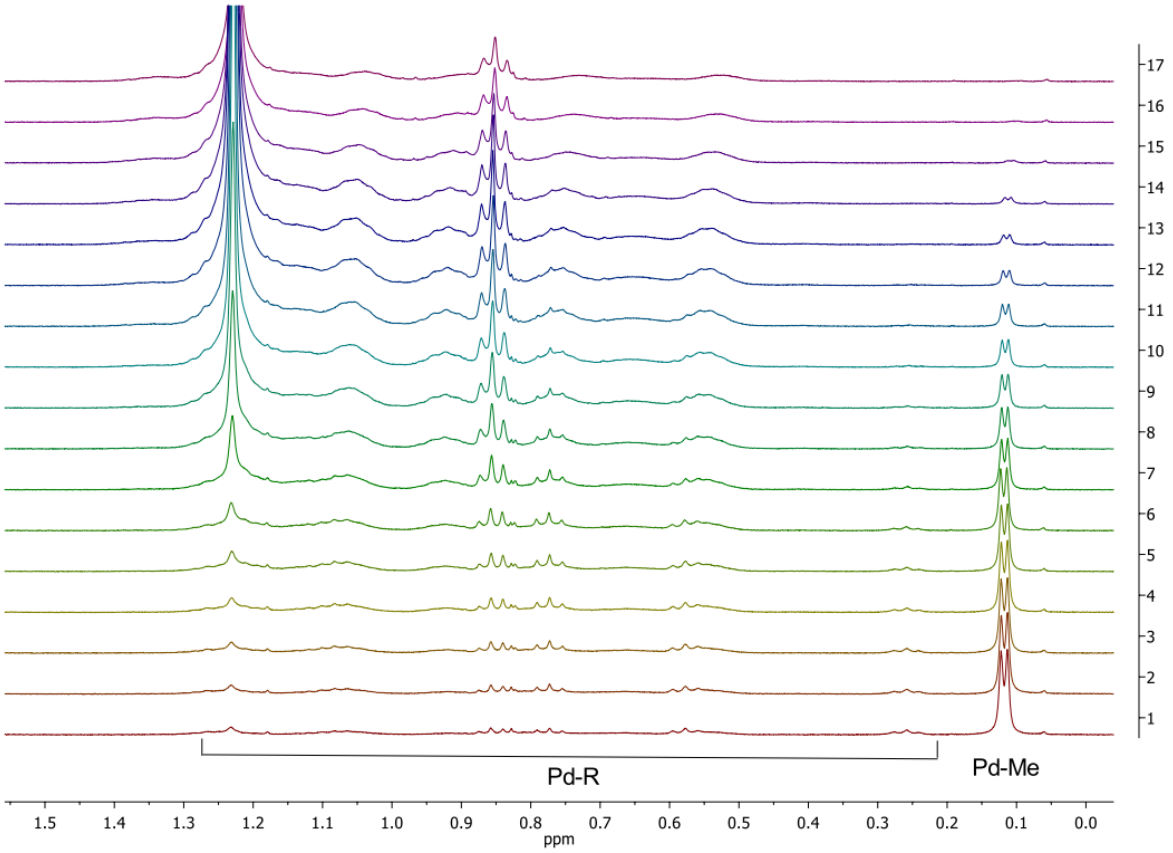


**Figure S16.** Consumption of Pd-*Me* by insertion of ethylene in **1-OPPh$_3$** and growth of Pd-polymeryl spezies ($^1$H-NMR, 400 MHz, $CD_2Cl_2$, -15 °C).

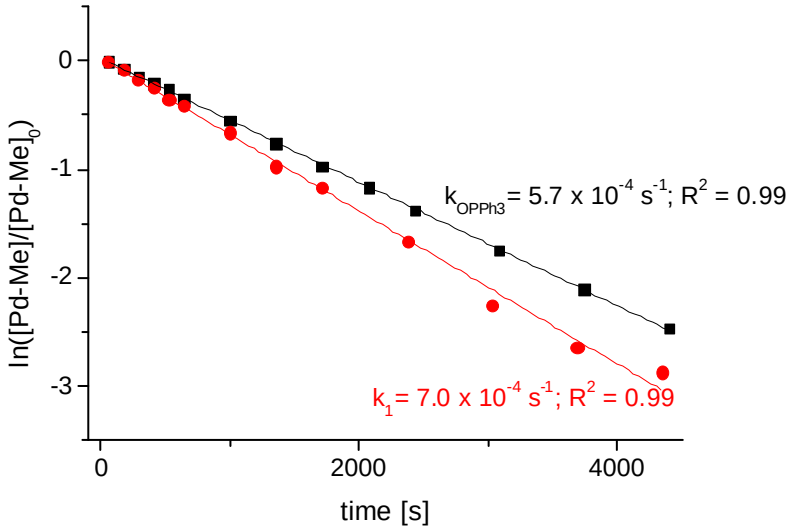


**Figure S17.** Pseudo first-order consumption of Pd-Me by insertion of MA, [Pd] = 0.0013 mol L$^{-1}$ in $CD_2Cl_2$ at -15 °C

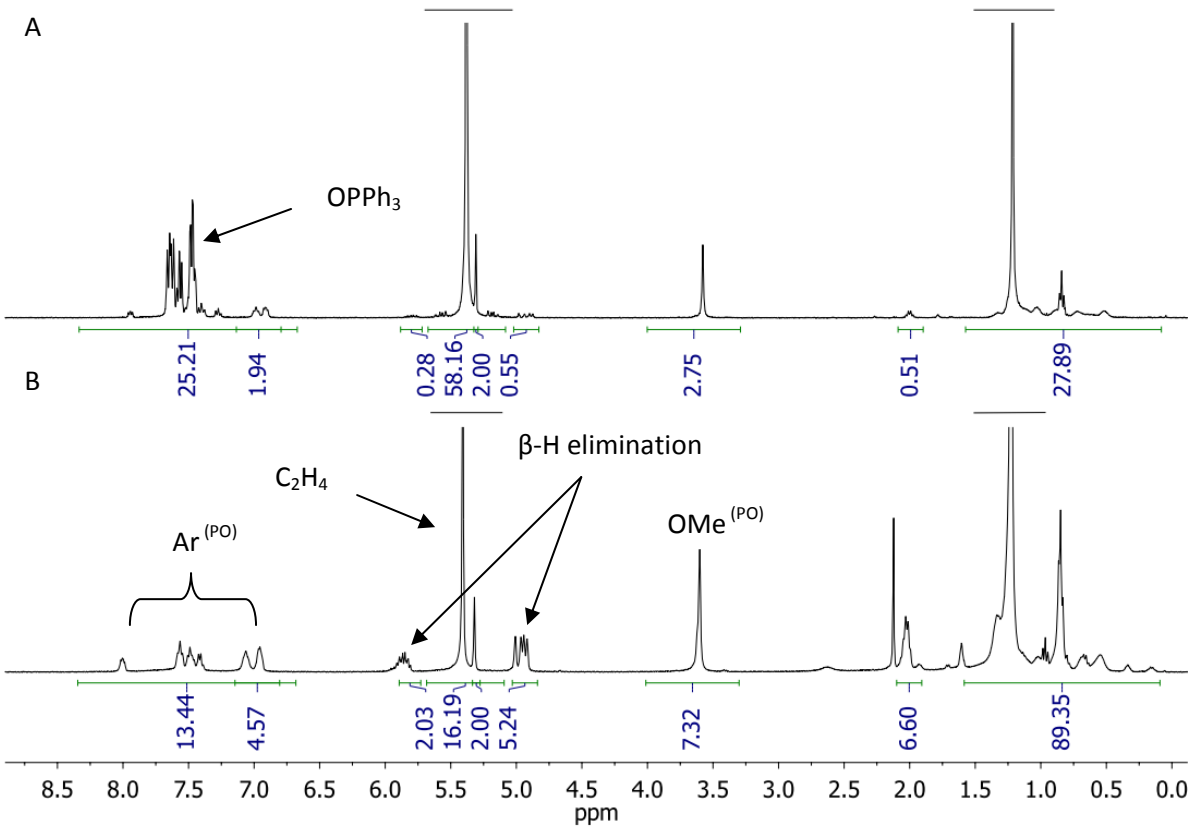


**Figure S18.** $^{1}$H-NMR spectrum (400 MHz, $CD_2Cl_2$, -15 °C) of ethylene insertion into **1-OPPh$_3$** (A) and **1** (B) after ~140 min.

## IX. Methyl Acrylate Insertion Kinetic

The insertion of MA into the Pd-Me bond of (P^O)PdMe (**1**) and the subsequent insertion of a second equivalent of MA was monitored by $^1$H-NMR for **1-OPBu$_3$, 1-OPPh$_3$**, **1-dmso**, and *in situ* generated **1** ([{(**1-Cl**)-μ-Na}$_2$] + $AgBF_4$ → **1** + AgCl ↓ + $NaBF_4$↓) under pseudo first order conditions.

General Procedure: To a solution of [(P^O)PdMe(L)] in $CD_2Cl_2$ (0.02 M) containing 1,1,1,2-tetrachloroethane as internal reference were added 14 equiv of MA. For kinetic analysis of *in situ* generated **1**: To a mixture of [{(**1-Cl**)-μ-Na}$_2$], 1.1 equiv $AgBF_4$ was added $CD_2Cl_2$ (~0.02M, Pd:MA = 1:19), the suspension was shaken for 1 minute and then filtered to give a clear catalyst solution. For determination of the rate constants for the first insertion the disappearance of the Pd-*Me* shift and for the second insertion the disappearance of the resulting Pd-CH(C(O)OMe)$CH_2$*Me* shift were analyzed (Figure S19).

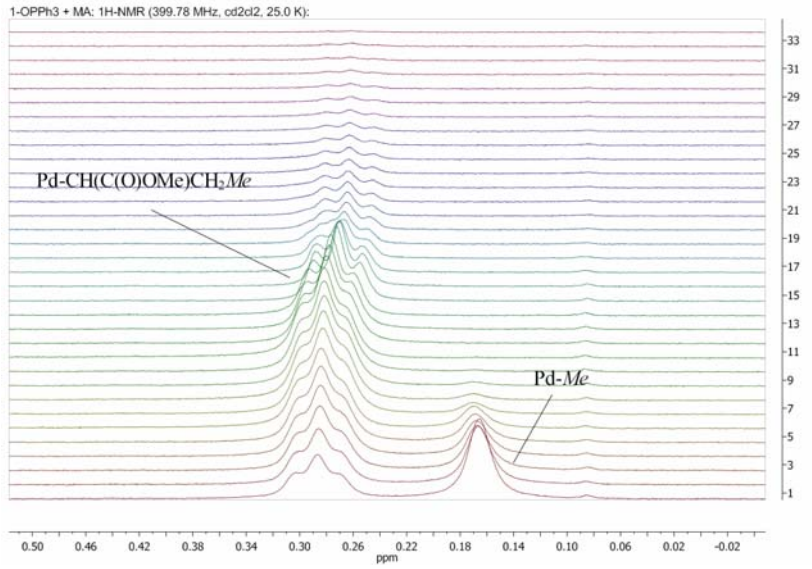


**Figure S19.** Consumption of Pd-*Me* and subsequently of Pd-CH(C(O)OMe)$CH_2$*Me* by insertion of MA in **1-OPPh$_3$** ($^1$H-NMR, 400 MHz, CD2Cl2, 25 °C).

## X. References


(1) Armarego, W. L.; Perrin, D. D. *Purification of Laboratory Chemicals*; 4th ed.; Elsevier: Burlington, 1996.
(2) De Graaf, W.; Boersma, J.; Smeets, W. J. J.; Spek, A. L.; Van Koten, G. *Organometallics* **1989**, *8*, 2907-2917.
(3) Salo, E. V.; Guan, Z. *Organometallics* **2003**, *22*, 5033-5046.
(4) Drent, E.; Dijk, R. v.; Ginkel, R. v.; Oort, B. v.; Pugh, R. I. *Chem. Commun.* **2002**, 964-965.
(5) Guironnet, D.; Roesle, P.; Rünzi, T.; Göttker-Schnetmann, I.; Mecking, S. *J. Am. Chem. Soc.* **2009**, *131*, 422-423.
(6) Rünzi, T.; Guironnet, D.; Göttker-Schnetmann, I.; Mecking, S. *J. Am. Chem. Soc.* **2010**, *132*, 16623-16630.
(7) Cotton, F. A.; Barnes, R. D.; Bannister, E. *J. Chem. Soc.* **1960**, 2199-2203.
(8) Guironnet, D.; Caporaso, L.; Neuwald, B.; Göttker-Schnetmann, I.; Cavallo, L.; Mecking, S. *J. Am. Chem. Soc.* **2010**, *132*, 4418-4426.
(9) Vela, J.; Lief, G. R.; Shen, Z.; Jordan, R. F. *Organometallics* **2007**, *26*, 6624-6635.
(10) Stoe, *X-RED version 1.3, Data Reduction Program,* Darmstadt, Germany, **2005**.
(11) Sheldrick, G. M. *SHELXS-97, Program for Crystal Structure Analysis*; Universität Göttingen: Göttingen, 1986.
(12) Sheldrick, G. M. *SHELXL-97, Program for Crystal Structure Refinement*; Universität Göttingen: Göttingen, 1997.
(13) Brandenburg, K. *Diamond version. 3.1,*; Crystal Impact GbR: Bonn, 2005.
(14) Savitzky, A.; Golay, M. J. E. *Analyt. Chem.* **1964**, *36*, 1627-1639.